

Chemical Papers

A Spectrophotometric and DFT study of the behavior of 6-bromoquercetin in aqueous solution --Manuscript Draft--

Manuscript Number:	
Full Title:	A Spectrophotometric and DFT study of the behavior of 6-bromoquercetin in aqueous solution
Article Type:	Original Paper
Section/Category:	Analytical Chemistry and Spectroscopy
Funding Information:	
Abstract:	Acid-base activity, keto-enol tautomerism and complexing properties of 6-bromoquercetin are investigated in water media at different conditions. The constants of dissociation (pKa) have been determined in pH region at various ionic strength. The analysis of protonation process is conducted in strongly acidic solutions of HCl. The complexation were studied with trivalent lanthanides. The stability constant of monocomplex species ML (M(III) =Ce, Pr, Nd, Sm, Eu, Gd, Tb, Dy, Er, Tm, Yb, Lu) have been obtained. For interpretation and verification of received data the DFT calculations were implemented.
Corresponding Author:	Maxim A. Lutoshkin, Ph.D. Institute of chemistry and Chemical Technology SB RAS Krasnoyarsk, RUSSIAN FEDERATION
Corresponding Author Secondary Information:	
Corresponding Author's Institution:	Institute of chemistry and Chemical Technology SB RAS
Corresponding Author's Secondary Institution:	
First Author:	Maxim A. Lutoshkin, Ph.D.
First Author Secondary Information:	
Order of Authors:	Maxim A. Lutoshkin, Ph.D. Vladimir A. Levanskiy, Dr.Sci. Sergey V. Baryshnikov, PhD
Order of Authors Secondary Information:	
Author Comments:	-
Suggested Reviewers:	Jing Zou zoujing@hqu.edu.cn published similar research D. V. Snigur, PhD Mechnikov Odessa National University, Odessa, Ukraine denis270892@yandex.ru published similar studies Marta Arczewska Department of Biophysics, University of Life Sciences in Lublin, Akademicka 13, 20-950 Lublin, Poland marta.arczewska@up.lublin.pl Published similar research

[Click here to view linked References](#)

1 **A Spectrophotometric and DFT study of the behavior of 6-bromoquercetin**
2 **in aqueous solution**

3
4 **Maxim A. Lutoshkin^{1,2*}, Vladimir A. Levdanskiy², Sergey V. Baryshnikov² and Boris N.**
5 **Kuznetsov^{2,3}**

6
7 ¹ *Université de Lyon, Université Claude Bernard Lyon 1, CNRS, UMR 5256, IRCELYON,*
8 *Institut de recherches sur la catalyse et l'environnement de Lyon, Villeurbanne, France*

9
10 ² *Institute of Chemistry and Chemical Technology SB RAS, Federal Research Center,*
11 *“Krasnoyarsk Science Center SB RAS”, Krasnoyarsk, Russian Federation*

12
13 ³ *Institute of Non-Ferrous Metals and Materials Science, Siberian Federal University,*
14 *Krasnoyarsk, Russian Federation*

15
16 *Corresponding author, e-mail: maximsfu@yahoo.com

17
18 Received [Dates will be filled in by the Editorial office]

19
20
21
22
23
24
25
26
27
28
29
30
31
32
33
34
35
36
37
38
39
40
41
42
43
44
45
46
47
48
49
50
51
52
53
54
55
56
57
58
59
60
61
62
63
64
65

Abstract

Acid-base activity, keto-enol tautomerism and complexing properties of 6-beomoquercetin are investigated in water media at different conditions. The constants of dissociation (pKa) have been determined in pH region at various ionic strength. The analysis of protonation process is conducted in strongly acidic solutions of HCl. The complexation were studied with trivalent lanthanides. The stability constant of monocomplex species ML (M(III) = Ce, Pr, Nd, Sm, Eu, Gd, Tb, Dy, Er, Tm, Yb, Lu) have been obtained. For interpretation and verification of received data the DFT calculations were implemented.

Keywords: DFT, Flavonoids, Lanthanide, Spectrophotometric.

Introduction

Being secondary metabolites, flavonoids exist ubiquitous in the plant world (Panche et al. 2016). Quercetin or 5,7,3',4'-flavon-3-ol is the most known and studied ligand from this group of chemicals. The various qualities, such as anticancer (Le Marchand 2002), antibacterial (Cushnie and Lamb, 2005) and antidiabetic (Vinayagam and Xu 2015) activities demonstrate a multifaceted nature of quercetin. The numerous derivatives of quercetin are also show notable biochemical characteristics (Kessler et al 2003; Sotnikova et al 2013; Manach et al 1998). The complexes of flavonoids with all of groups of metals (Kasprzak et al. 2015; Samsonowicz and Regulska 2017) are described in literature primarily for solid-state conditions.

The flavonoids exhibit medical and biological properties in water. Nevertheless, the low solubility make them problematic objects for study of standard physical-chemical methods. The solubility of quercetin in H₂O at room temperature is about 10⁻⁴ M (Srinivas et al. 2010). In the same time, the necessary concentration for NMR-analysis or potentiometric study is 10⁻²-10⁻¹ M. In all works where the issue of flavonoids in solution has been discussed the water-ethanol mixtures or non-aqueous liquids were used as solvent. However, under such conditions the behaviour of flavonoids is fundamentally different from biological media. The spectrophotometric technique is one of the few methods that allow to research small amount of sparingly soluble compounds and determine all equilibrium parameters in pure water with concentration <10⁻⁴ M.

The rare-earth elements (REEs) have the typical characteristics of trivalent metals in solution and suitable for consideration as the modelling systems. In addition, the data for linkages lanthanides with flavonoids can be used for extraction and separation of REEs. The goal of current research was to exploring of acid-base, keto-enol and metal bonding processes of 6-bromoquercetin and demonstrate that the halogen derivatives of flavonoids is also display the useful properties in solution.

Theoretical

The values of dissociation constant (pK_a) have been calculated using equation (Leggett 1985):

$$A_i = \frac{C_{HL}(\varepsilon_L \cdot K_a + \varepsilon_{HL}[H^+])}{K_a + [H^+]}, \quad (1)$$

with the Henderson-Hasselbach equation (Tiwari and Ghosh 2010):

$$pH = pK_a + \log(IR); \quad IR = \frac{A_i - A_{HL}}{A_L - A_i}, \quad (2)$$

where IR - ionization ratio.

The non-linear Cox–Yates method (Cox 1983) based on the excess acidity function χ (Cox 1981) was used to determine the protonation constant (K_H) in strongly acidic solutions:

$$A_i = \frac{A_{HL} - A_{H_2L^+}}{1 + \left(\frac{C_{H^+}}{K_H}\right)10^{(m*\chi)}} + A_{H_2L^+}; \quad (3)$$

where A_i , A_{HL} (ε_{HL}), $A_{H_2L^+}$ ($\varepsilon_{H_2L^+}$), and A_L (ε_L) are the absorbances and molar extinction coefficients of the process solution, the free ligands, and its conjugate acid or base, respectively. Conditional stability constants (K') for monocomplex species were calculated from the equations 1-2 (Grebenyuk et al. 2015):

$$A_{calc}^\lambda = \varepsilon_{HL}^\lambda (C_{HL} - [ML]) + \varepsilon_M^\lambda (C_M - [ML]) + \varepsilon_{ML}^\lambda [ML], \quad (4)$$

$$[ML] = \frac{1}{2} \left[\left(\frac{1}{K'} + C_{HL} + C_M \right) + \sqrt{\left(\frac{1}{K'} + C_{HL} + C_M \right)^2 - 4C_M C_{HL}} \right], \quad (5)$$

where A_{calc}^λ is an absorbance at a given wavelength and C_M and C_{HL} were analytical concentrations of lanthanides and ligand, respectively. The ε^λ is a value of molar extinction coefficient at single wavelength. The optimal values for K' , K_a and K_H and ε^λ were found from the least squares analysis (Leggett 1985):

$$f(C_M, C_L, K', \varepsilon_i) = \sum_{i=1}^n (A_i^\lambda - A_i^{calc})^2 \xrightarrow{K, \varepsilon_i} \min. \quad (6)$$

83 Calculations of all equilibrium constants and molar extinction coefficients were performed
 84 using Wolfram Mathematica (<http://www.wolfram.com/>).

85 The quantum-chemical computations were performed using the GAMESS US (Schmidt
 86 1993) program package on the cluster MVS-1000M of the Institute of computational modeling
 87 SB RAS. Geometry optimization was performed by density functional theory (DFT) with seven
 88 functionals: PBE0 (Adamo and Barone 1999) (under Grimme's empirical correction (Grimme
 89 et al. 2010)), revTPSS (Perdew et al. 2011), M06-2L; M06; M06-2X; M06-HF (Zhao and
 90 Truhlar 2008) and CAM-B3LYP (Yanai and Tew 2004). The cc-pVDZ (Dunning 1989) basis
 91 set functions was applied at C, H, O and Br atoms. The solvent effects were evaluated using the
 92 SMD solvation model (Marenich et al. 2009). The calculation of equilibrium constants were
 93 performed by following equation (Bryantsev et al. 2008):

$$\log K^{\text{calc.}} = -\Delta\Delta G^{\text{solv.}} / (2.303RT) \quad (7)$$

$$\Delta\Delta G^{\text{solv.}} = \Delta G^{\text{gas}} + \Delta G^{\text{aq.}} + \Delta E^{\text{zpe}} - E^{\text{corr.}} \quad (8)$$

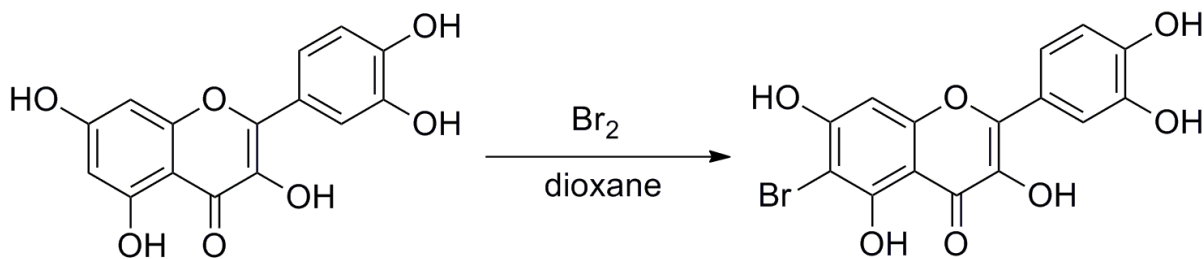
98 , where

$$E^{\text{corr.}} = RT \ln([H_2O]) = 9.964 \text{ kJ/mol.} \quad (9)$$

101 Here, $RT \ln([H_2O])$ is a free energy change associated with moving a solvent from a standard-
 102 state solution phase concentration of 1 M to a standard state of the pure liquid, 55.34 M
 103 (Vukovic et al. 2015). The change of Gibbs free energy in solid state and in solution (ΔG^{gas} and
 104 $\Delta G^{\text{aq.}}$). E^{zpe} is calculated harmonic vibrational frequencies to estimate the zero point energy
 105 correction.

107 Experimental

109 The UV-Vis spectra were measured with Leki SS2109-UV scanning spectrophotometer (Leki
 110 Instruments, Finland) using 1 cm quartz cells. Cell thermostating (± 0.1 K) was performed with
 111 the Haake K15 thermostat connected to the Haake DC10 controller. All measurements were
 112 performed at 298 K. The synthesis of bromine derivative of quercetin was performed by the
 113 simple method described at (Nagimova et al. 1996): 1g of quercetin was brominated in dioxane
 114 at 298 K without stirring (Scheme 1). The precipitated orange crystals were washing with water
 115 and crystallize three times from ethanol. The test by paper chromatography have been
 116 demonstrate the absence of initial quercetin in the final products.



117

118 **Scheme 1.** The synthesis of 6-bromoquercetin.

119

120 *Materials*

121

122 *Chemicals*

123 All chemicals were of analytical grade: quercetin (Aldrich $\geq 95\%$, HPLC), CH_3COONa ,
 124 CH_3COOH , citric acid, TRIS, Na_2HPO_4 , glycine, Br_2 , NaClO_4 , HCl , $\text{LnCl}_3 \cdot 6\text{H}_2\text{O}$ ($\text{Ln} = \text{Ce}, \text{Pr},$
 125 $\text{Nd}, \text{Sm}, \text{Eu}, \text{Gd}, \text{Tb}, \text{Dy}, \text{Er}, \text{Tm}, \text{Yb}$). All stock solutions were obtained by dissolution of dry
 126 salts and ligand weights. The solutions of bromquercetin were prepared from its ethanol
 127 concentrated solution ($C = 6 \cdot 10^{-3} \text{ M}$). The concentration of ethanol did not exceed 1% in the final
 128 solution. Buffer solutions within the pH range from 1.80 to 3.60 were prepared with glycine
 129 and HCl , from 3.60 to 5.60 with CH_3COOH and CH_3COONa (for study of complexation), from
 130 3.60 to 7.00 with citric acid and Na_2HPO_4 (for study of dissociation), from 7.00 to 8.60 with
 131 TRIS and HCl . The accurate desired pH values were obtained by adjusting the molarities of the
 132 buffer components in suitable amounts. The accurate concentration of Ln^{3+} has been establish
 133 by complexometric titration with EDTA.

134

135

136

136 **Results and discussion**

137

138 3.1 The study of acid-base properties

139 The various states of investigated flavonoid have the different shape of electronic
 140 spectra. Fig. 1 demonstrate the spectra of neutral, protonated and monoanionic forms of
 141 quercetin and 6-bromoquercetin. In Table 1 represent the position of absorption maximum for
 142 bromoquercetin compared with pure quercetin. There is linear relationship between optical
 143 density and concentration for all forms of BQR. Thus, the formation of ionic associate or dimers
 144 are not taking place. The interaction between components of used buffers and ligand is not find.

145 It is seen that for BQR spectra all peaks are shifted in long-wave region with respect to
 146 peaks of quercetin.

1
2
3
4
5
6
7
8
9
10
11
12
13
14
15
16
17
18
19
20
21
22
23
24
25
26
27
28
29
30
31
32
33
34
35
36
37
38
39
40
41
42
43
44
45
46
47
48
49
50
51
52
53
54
55
56
57
58
59
60
61
62
63
64
65

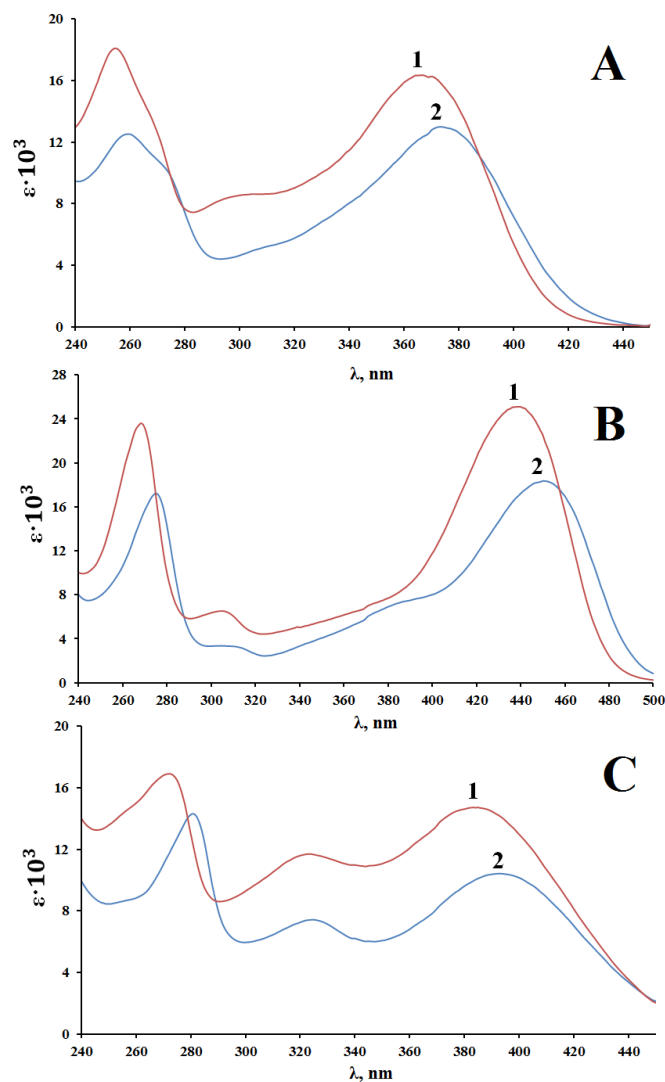
147 **Table 1.** The values of wavelength (nm) of main absorbance peaks of BQR and quercetin

148

Form	6-Bromoquercetin		Quercetin	
	$\lambda^{\max, 1}$	$\lambda^{\max, 2}$	$\lambda^{\max, 1}$	$\lambda^{\max, 2}$
Neutral	256	373	255	367
Protonated	275	450	268	439
Monoanionic	281	393	272	383

149

150 The molar extinction coefficients is less for bromine derivative. At pH above 8.20 the
 151 destruction of BQR is observed. For this reason the acid-base properties of bromoquercetin
 152 were investigated in pH region from 2.0 to 7.3, where occurring only first step of dissociation.
 153 All raw spectroscopic data are given in the Supplementary Material (Tables S1-S6).



154

155 **Fig. 1.** The UV-vis spectra of different forms of quercetin(1) and 6-bromoquercetin(2):
 156 neutral at pH=1 (A), protonated at C(HCl)>10 M (B) and monoanionic (C) at pH=8.0.

1
2
3
4
5
6
7
8
9
10
11
12
13
14
15
16
17
18
19
20
21
22
23
24
25
26
27
28
29
30
31
32
33
34
35
36
37
38
39
40
41
42
43
44
45
46
47
48
49
50
51
52
53
54
55
56
57
58
59
60
61
62
63
64
65

157 As the derivative of quercetin, 6-bromoquercetin exhibit property of a weak acid. Fig. 2
 158 provides the spectral change of BQR as function of pH. The presence of isosbestic points
 159 reflects the transformation only one form in single product. As a background electrolyte was
 160 utilized NaClO₄. The slight absorption of phosphate-citrate buffer was take into account in
 161 calculations of final values of pK_a. The obtained results of acid-base properties in pH region
 162 are given at Table 2. The constant of dissociation was determine at three values of ionic
 163 strength: 0.1, 0.5 and 1.0 M.

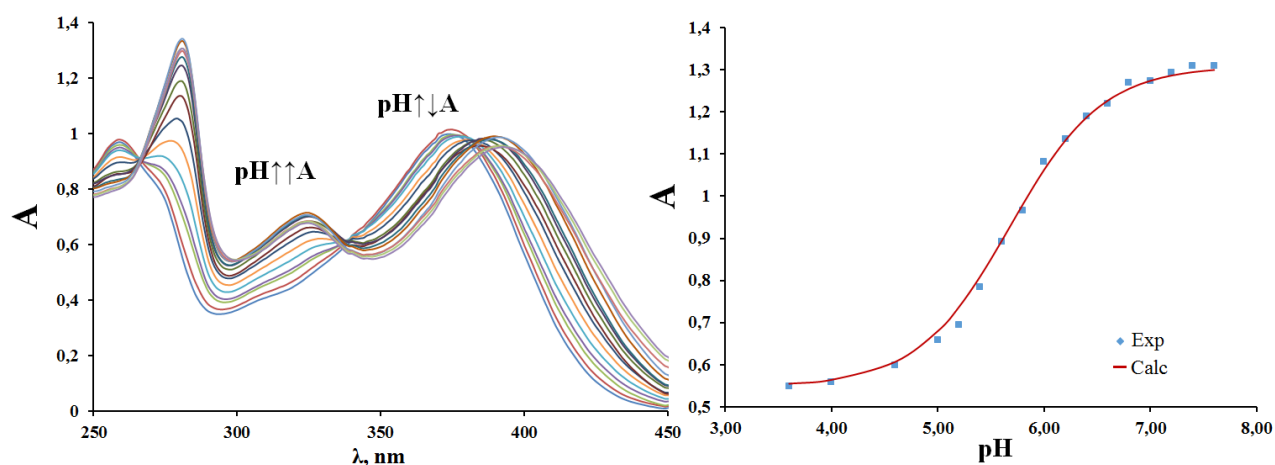
164

165 **Table 2.** The values of pK_a, extinctions of anionic and neutral form of BQR

I (NaClO ₄)	0.1		0.5		1.0	
λ, nm	281	408	281	408	281	408
pK _a ± 0.02	5.68	5.70	5.85	5.90	6.04	6.01
log(ε _L) ± 0.01	4.16	3.96	4.14	3.94	4.14	3.93
log(ε _{HL}) ± 0.01	3.78	3.60	3.78	3.61	3.79	3.62

166

167 This has been done in order to use these data in various conditions. For three values of
 168 pK_a the analysis of log(IR)-pH relationship (eq. 2; Fig. S1) demonstrate the mono deprotonation
 169 character of during process. The founded values of pK_a of BQR lie from 5.68 to 6.04
 170 logarithmic units. All these data characterize 6-bromoquercetin as more acidic ligand than
 171 quercetin (pK_a = 7.20 (Kopacz 2003)). This fact can be explain by polarizing effect inducted
 172 by bromine atom: the appearance in molecular structure heavy halogen atom is increase of
 173 electrostatic tension and weaken of O-H bond.



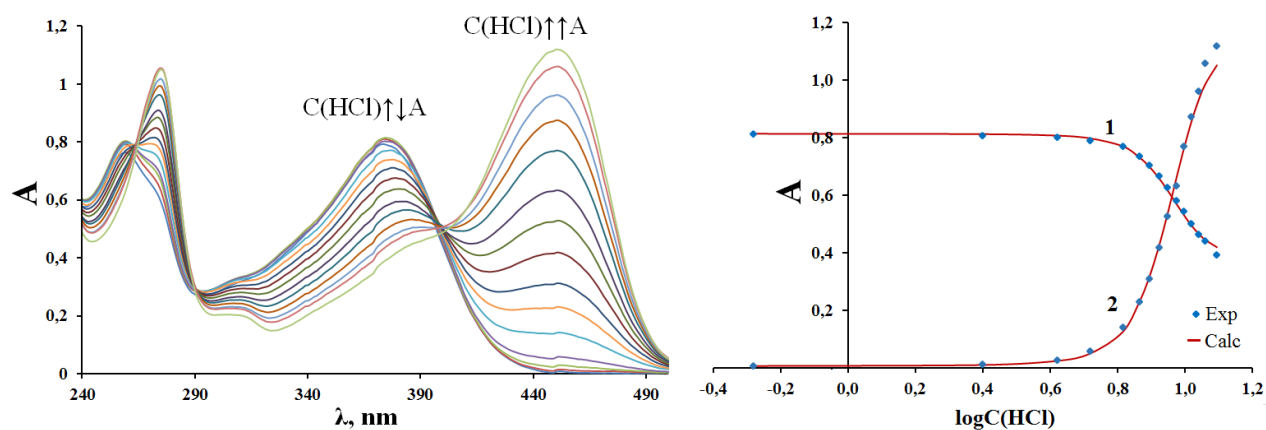
174

175

176 **Fig. 2.** The UV-Vis spectra and absorbance at 281 nm of 6-bromoquercetin at various values
 177 of pH; C(bromoquercetin) = 9.14 · 10⁻⁵ M, I = 0.1 M.

61
62
63
64
65

178 The treatment of acid-base properties in acidic media was performed in concentrated
 179 hydrochloric solutions. Fig. 3 has shown a transformation of BQR spectra at increase of HCl
 180 concentration. The calculations of protonation constant ($-\text{p}K_{\text{H}}$) have been carried out for 2
 181 wavelength – 450 and 375 nm. For both wavelength the assessment provides the equal values
 182 of $-\text{p}K_{\text{H}} = 3.50 \pm 0.03$ logarithmic units. An analogous value for quercetin is 2.30 log units
 183 (Kopacz 2003). Therefore, the reported value of $-\text{p}K_{\text{H}}$ describes this flavonoid as a weaker base
 184 in acidic solution than quercetin. The m^* parameter (from eq. 3) or solvation coefficient t
 185 (Hoyuelos et al. 2005) for this process is equal 0.97 ± 0.04 . This coefficient depends on the
 186 mechanism of protonation and nature of protonated atom. In this case ($m^* \sim 1$) it indicates that
 187 H_2L^+ form of BQR is small and not very polarizable molecule (Hoyuelos et al. 2005).



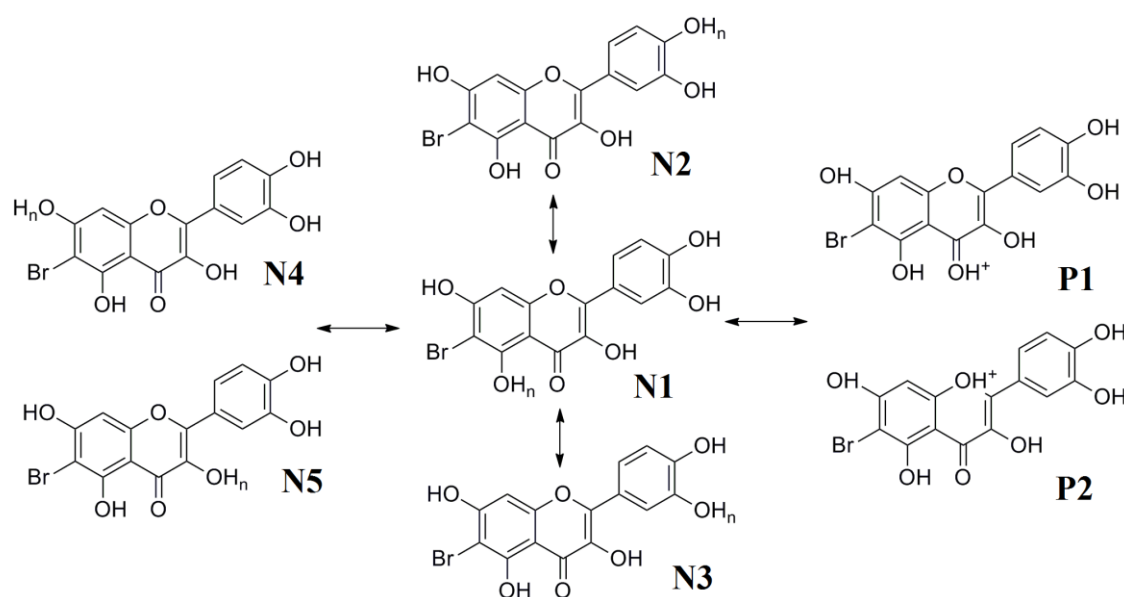
189 **Fig. 1.** The UV-vis scanning spectra of BQR obtained at various concentration of HCl and
 190 absorbance (1 – 375 nm; 2 – 450 nm) as a function of $\log(\text{C}(\text{HCl}))$; $\text{C}(\text{bromoquercetin}) =$
 191 $6.09 \cdot 10^{-5}$ M.

193

194 3.1 The DFT study

195 The dissociation and protonation of neutral form of BQR can lead to the appearance of several
 196 tautomers. Each of OH group in this molecule can dissociate or be protonated. The all possible
 197 isomers of anionic and protonated forms are collected at Scheme 2.

198
199
200
201
202
203
204
205
206
207
208
209
210
211
212
213
214
215
216
217
218
219
220
221
222
223
224
225
226
227
228
229
230
231
232
233
234
235
236
237
238
239
240
241
242
243
244
245
246
247
248
249
250
251
252
253
254
255
256
257
258
259
260
261
262
263
264
265



198

199

200 **Scheme 2.** The anionic ($n=0$) and protonated ($n=2$; P1 and P2) tautomers of BQR

201

202 The tautomers P1 and P2 are possible only for protonated form. For the estimate of
 203 thermodynamic stability of these structures the absolute and relative energies were calculated
 204 (Table 3) at level $cc\text{-}p\text{VDZ}/\text{DFT}/\text{PBE0}/\text{SMD}$. All assessments demonstrate that acid-base
 205 processes relate with 4-carbonyl and 5-hydroxyl groups. The most stable anionic form is the
 206 isomer with negative charge on the 5-hydroxyl position (N1). The domination form of
 207 protonated bromoquercetin is the cation P1 with one more proton atom on the 4-carbonyl group.

208

209 **Table 3.** The calculated absolute (a.u.) and relative ($\text{kJ}\cdot\text{mol}^{-1}$) energies of BQR tautomers

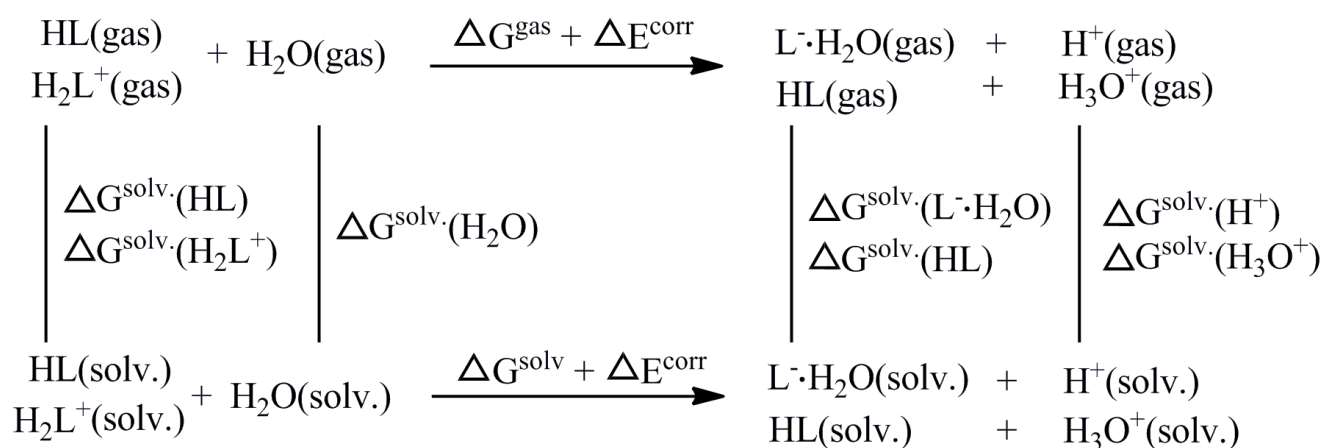
210

Tautomer	Protonated form ($n=2$)		Anionic form ($n=0$)	
	Absolute energy	Relative energy	Absolute energy	Relative energy
N1	-3676.724254	92.19	-3675.946043	0.00
N2	-3676.740029	50.77	-3675.931125	39.17
N3	-3676.740148	50.46	-3675.931271	38.78
N4	-3676.747360	31.53	-3675.922961	60.60
N5	-3676.737160	58.31	-3675.937402	22.69
P1	-3676.759367	0.00		
P2	-3676.711874	124.69		

211

212 Now, the quantitative analysis of the Lowdin's charges can help to explain the difference of
 213 acid-base properties between quercetin and BQR. The charge of O-atom of 5-hydroxyl group
 214 is -0.304 and -0.272 for quercetin and bromoquercetin, respectively. The charge of hydrogen is
 215 the same for both cases. Thus, bromine to decrease of negative charge on oxygen atom and
 216 reinforces the repulsion between H and O that lead to high acidity. Analogous reasons suited
 217 to protonation activates: the charge of 4-carbonyl oxygen is high for BQR (-0.291) than for
 218 quercetin (-0.307) and electrostatic bonding O-H is durable for quercetin.

219



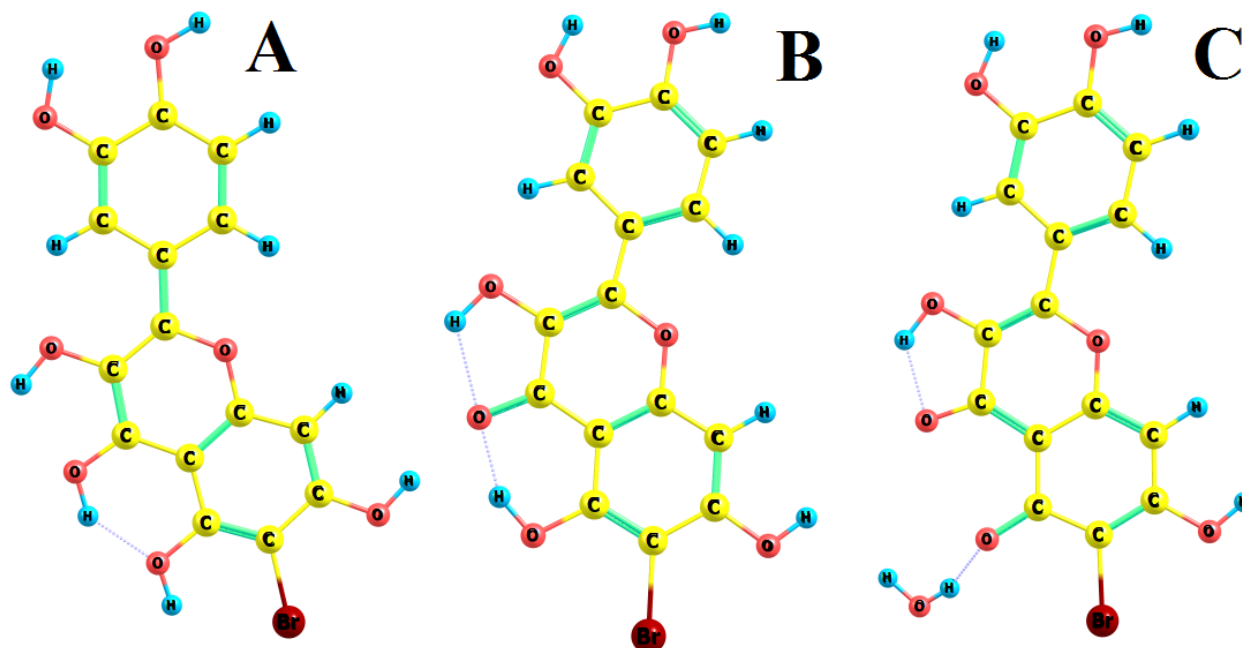
220

221

Scheme 3. The thermodynamic cycle for calculate $\text{pK}_a^{\text{calc.}}$ and $\text{pK}_H^{\text{calc.}}$.

222

223



224

225

Fig. 4. The optimization geometry of protonated (A), neutral (B) and anionic (C) forms.

226

1
2
3
4
5
6
7
8
9
10
11
12
13
14
15
16
17
18
19
20
21
22
23
24
25
26
27
28
29
30
31
32
33
34
35
36
37
38
39
40
41
42
43
44
45
46
47
48
49
50
51
52
53
54
55
56
57
58
59
60
61
62
63
64
65

227 For search of optimal DFT method to describe thermodynamic results ab initio
 228 calculations have been produced. The thermodynamic cycle showed at Scheme 3 was used for
 229 computation protocol. The obtaining of $\text{pK}_a^{\text{calc.}}$ and $\text{pK}_H^{\text{calc.}}$ has been carried out at level cc-
 230 pVDZ/DFT/SMD with using seven density functional. The cc-pVDZ has established itself as
 231 usable for estimate of equilibrium processes of heterocyclic compounds (Lutoshkin and
 232 Kazachenko 2017). The functionals from minesota family, TPSS group and LYP-class were
 233 tested in this work. This choice was based on the wide using of these functionals for calculate
 234 of various equilibrium processes (Banerjee and Bhanja 2018). Guided by theoretical work
 235 (Bishnu and Schlegel 2016) the explicit water molecule was applied for compilation of $\text{pK}_a^{\text{calc.}}$.
 236 The optimization geometry of studied species demonstrated at Fig. 4. The findings of estimation
 237 are given at Table 4. In our case, the better approximation (for dissociation process) provides
 238 functional M06-HF with 100% of Hartree-Fock exchange. PBE0 demonstrate the best approach
 239 for pK_a . All of other functionals gives grater discrepancy with experimental data.

240

241 **Table 4.** The results of quantum-chemical simulation.

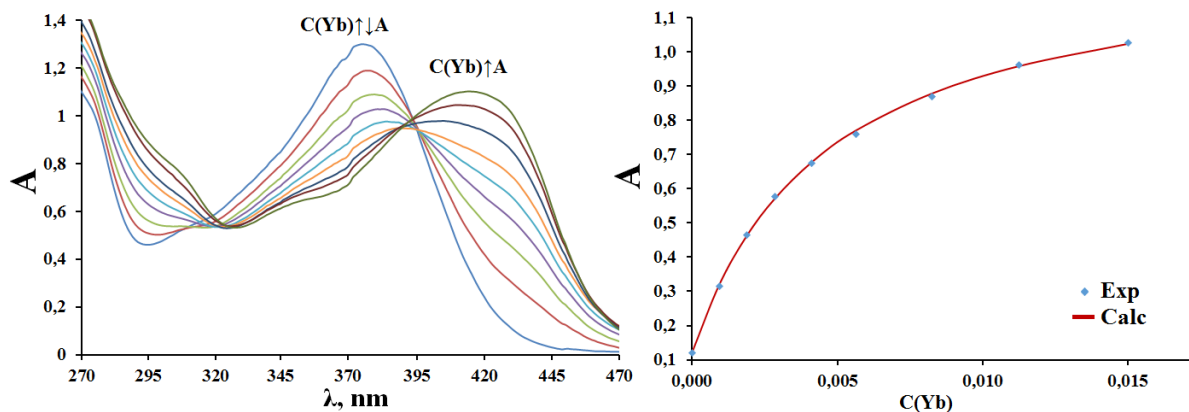
Density		Dissociation process			
Functional	$\Delta G^{\text{gas}} + \Delta G^{\text{solv.}}$, kJ/mol	ΔE^{ZPE}	$\text{pK}_a(\text{calc})$	$\text{pK}_a(\text{exp})$	
PBE0	91.23	-33.99	9.66		
revTPSS	104.79	-32.03	12.39		
M06-L	99.37	-34.05	11.08		
M06	82.97	-33.94	8.25	5.86	
M06-2X	82.71	-34.30	8.12		
M06-HF	65.30	-33.86	5.15		
CAM-B3LYP	117.59	-33.56	9.74		
Density		Protonation process			
Functional	$\Delta G^{\text{gas}} + \Delta G^{\text{solv.}}$, kJ/mol	ΔE^{ZPE}	$-\text{pK}_H(\text{calc})$	$-\text{pK}_H(\text{exp})$	
PBE0	-27.81	10.84	3.33		
revTPSS	-90.19	2.20	15.77		
M06-L	30.08	8.42	-6.39		
M06	31.35	7.70	-6.48	3.50	
M06-2X	25.39	7.91	-5.47		
M06-HF	-81.32	7.83	13.23		
CAM-B3LYP	26.81	-12.60	-2.13		

242

1
2
3
4
5
6
7
8
9
10
11
12
13
14
15
16
17
18
19
20
21
22
23
24
25
26
27
28
29
30
31
32
33
34
35
36
37
38
39
40
41
42
43
44
45
46
47
48
49
50
51
52
53
54
55
56
57
58
59
60
61
62
63
64
65

243 3.3 Stability of Lanthanide complexes

244 Bromoquercetin, as well as quercetin, is effective complexing agent for trivalent lanthanides in
 245 solution. All measurements were completed in acetate buffer at ionic strength 0.5 M. The
 246 working pH range lie from 4.40 to 5.40. Due to the studied flavonoid has small aqueous
 247 solubility, the determination of stability constants has been performed at constant concentration
 248 of ligand in each series. The various concentration of lanthanides was taken in excess
 249 ($C(M) > C(L)$) for eliminating the possibility of the formation of poly-ligand complexes M_nL_m .
 250 In Fig. 5, the BQR spectra under different concentration of ytterbium(III) are shown. For BQR-
 251 Ln(III) system ΔA^{\max} has a constant position at 430 nm (Fig. S2) and depends only from metal
 252 concentration. This facts, significant excess of Ln^{3+} and existence of a isopiestic points indicates
 253 about formation of one products – 1:1 complex ML. The similar reasons can be applied for all
 254 systems. The received data of equilibrium parameters for complexation are given at Table 3.



255

256

257 **Fig. 5.** The UV–Vis spectra and absorbance at single wavelength (429 nm) for Yb(III)-BQR
 258 system; $C(\text{bromoquercetin}) = 9.14 \cdot 10^{-5} \text{ M}$; $\text{pH} = 4.4$, $I = 0.5 \text{ M}$ (NaClO_4).

259

260 To confirm of chosen coordination model the stability constants for some of metals
 261 (Yb^{3+} and Er^{3+}) were obtain for three values of pH. The linear relationship of $\text{pH} - \log K$ and
 262 slope coefficient ≈ 1 testify to monodeprotonation of ligand upon complexation process.
 263 Furthermore, the formation of complexes with OH^- and acetate ions is typical for all rare earth
 264 metal. To take into account of side reactions the following equations were fitted:

265

$$K = \alpha_M \alpha_L K' \quad (10)$$

266

267

$$\alpha_M = 1 + \sum \beta_n [L]^n, \quad (11)$$

268

269

$$\alpha_L = 1 + \sum K_H [H^+], \quad (12)$$

60
61
62
63
64
65

270 where $K_H = 1/K_a$ was determine in pH region. The constants of adverse reaction (β_n)
 271 for $\text{Ln}(\text{OAc})_n$ and $\text{Ln}(\text{OH})^{2+}$ was taken from previously work (Lutoshkin et al. 2018) and given
 272 at Table S7.

273

274 **Table 5.** Conditional (K'), “true” (K) stability constants and value of extinction at 429 nm for
 275 BQR-Ln(III) systems

276

Ln(III)	pH \pm 0.01	log $K' \pm$ 0.01	log $\epsilon^{429} \pm$ 0.03	log $K \pm$ 0.05
Ce	5.20	2.18	4.14	4.04
Pr	5.20	2.31	4.14	4.83
Nd	5.20	2.13	4.17	4.27
Sm	5.20	2.59	4.12	4.91
Eu	5.40	2.72	4.13	4.83
Gd	5.20	2.64	4.14	4.82
Tb	4.60	2.43	4.15	5.50
Dy	4.60	2.24	4.16	5.27
	4.40	2.24	4.14	5.43
Er	4.60	2.40	4.18	5.40
	4.80	2.65	4.12	5.47
Tm	4.60	2.26	4.19	5.27
	4.20	2.12	4.14	6.40
Yb	4.40	2.34	4.15	6.42
	4.60	2.58	4.11	6.48
Lu	4.60	2.70	4.14	5.77

277

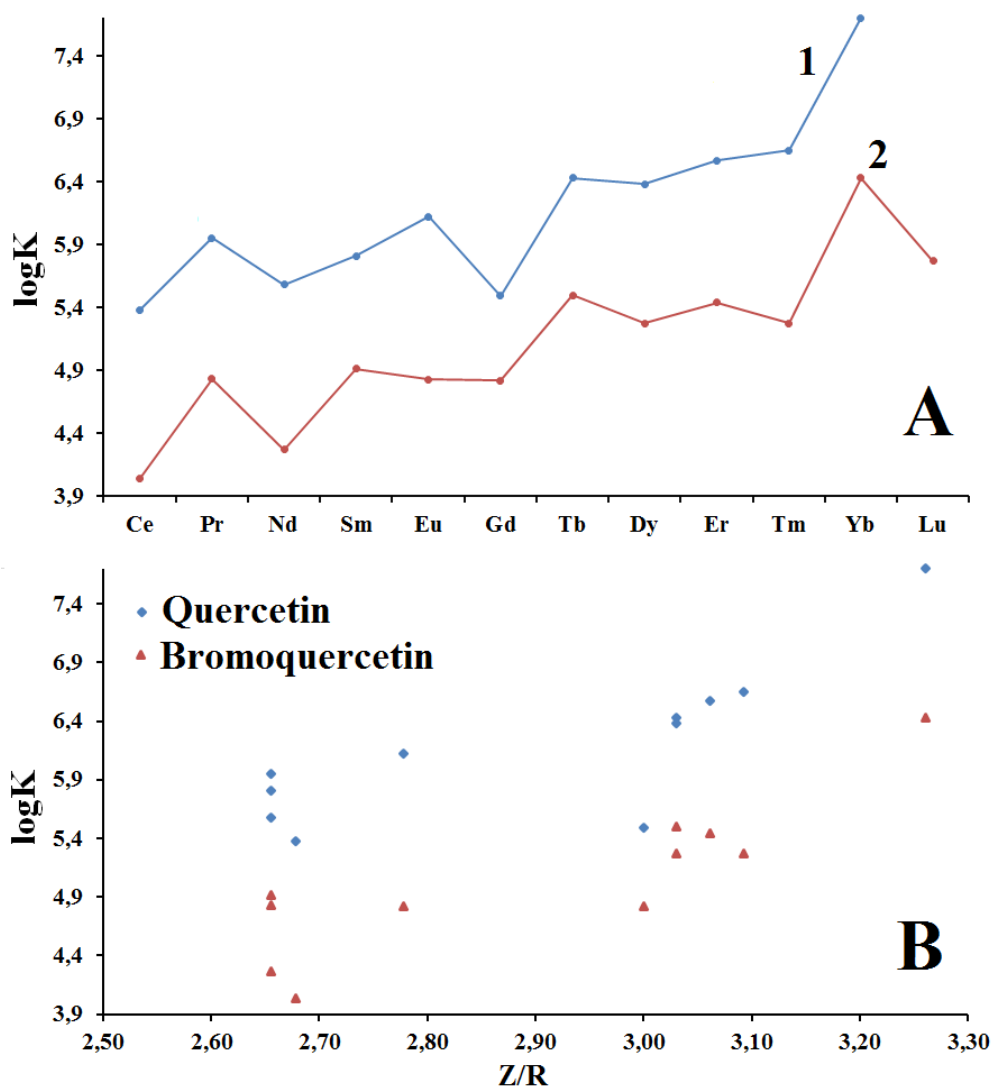
278 The obtained values of log K lie in region 4.0-6.5 logarithmic units. The stability
 279 constants follow the order: Ce<Nd<Gd \approx Eu \approx Pr<Sm<Dy \approx Tm<Er<Tb<Lu<Yb. Fig. 6 (A)
 280 illustrate Ln(III)-log K relationship. This shape of log K -Ln(III) curve indicate about general
 281 ionic nature of the bonding (Choppin 1983).

282

283 The similarity of spectral changes and molecular structure quercetin and BQR allows to
 284 propose the same coordination of their lanthanides complexes (via 3-hydroxyl-4-carbonyl
 285 group (Woźnicka et al. 2017; Lutoshkin et al. 2018)). Fig. 6(A) demonstrate that lanthanides
 286 complexes of BQR by 1-2 order weaker than Ln(III)-quercetin complexes. Like in the case of
 dissociation, this can be attributed to general electrostatic of molecule: the bromine atom

287 decrease the electronic density on the of 3-hydroxyl group and increase of decoupling between
 288 O atom of chelate group and Ln^{3+} .

289



290

291 **Fig. 6.** The logK-Ln(III) curves (A) for quercetin (1) and bromoquercetin (2) and logK-Z/R
 292 points (B).

293

294 The distribution of points on the logK-Z/R plot is presented on Fig. 6 (B) has shown
 295 that (as in the case of quercetin) all metals separated by two group: Ce-Eu and Gd-Lu. The
 296 second group of lanthanides show a weak correlation with ionic potential. This suggests that
 297 electrostatic interaction for these metals a slightly stronger than for Ce-Eu group. Perhaps, the
 298 separation can be explained by the sharp rise of covalence contribution in Gd-Lu complexes
 299 and participation of the 6d and/or 7s orbitals rather than f orbitals in the bonding (Choppin and
 300 Rizkalla 1994).

301

1
2
3
4
5
6
7
8
9
10
11
12
13
14
15
16
17
18
19
20
21
22
23
24
25
26
27
28
29
30
31
32
33
34
35
36
37
38
39
40
41
42
43
44
45
46
47
48
49
50
51
52
53
54
55
56
57
58
59
60
61
62
63
64
65

Conclusions

The thermodynamic parameters of 6-bromoquercetin have been described in solution using electronic absorption spectroscopy. The spectral, acid-base and complexing properties were studied at various ionic strength and acidity. Bromoquercetin is a stronger acid ($pK_a=5.68-6.04$) and weak base ($-pK_H=3.50$) than quercetin.

At level cc-pVDZ/DFT/PBE0/SMD were suggests the dominated forms (neutral, monoanionic and protonated) of BQR and explain their acidity. Seven density functionals (PBE0, CAM-B3LYP, M06, M06-L, M06-2X, M06-HF and revTPSS) were tested for search an optimal theoretical pathways to describe of obtained data. M06-HF and PBE0 functionals provide the better approximation for dissociation and protonation processes, respectively. The computation protocol with explicit water and specific solvation has been allows to reproduce experimental values with discrepancies ± 0.5 logarithmic units.

The investigation of 1:1 complexes of bromoquercetin and 12 lanthanides has been perform at wide range of pH at constant ionic strength ($I = 0.5$ M). 16 conditionals and 12 “true” equilibrium stability constants were obtained. The received stability constants lie from 4.04 to 6.46 logarithmic units and increase in the following order: Ce<Nd<Gd \approx Eu \approx Pr<Sm<Dy \approx Tm<Er<Tb<Lu<Yb. The low efficiency of BQR as complexation agent (compared to quercetin) was explain by the distribution of charges in optimization structure.

References

- Adamo C, Barone V (1999) Toward reliable density functional methods without adjustable parameters: The PBE0 model. *J Chem Phys* 110:6158-6170. doi: 10.1063/1.478522
- Banerjee S, Bhanja SK, Chattopadhyay PK (2018) Quantum chemical predictions of aqueous pK_a values for OH groups of some α -hydroxycarboxylic acids based on ab initio and DFT calculations. *Computational and Theoretical Chemistry* 1125:29-38.
- Bishnu T, Schlegel HB (2016) Density Functional Theory Calculation of pK_a 's of Thiols in Aqueous Solution Using Explicit Water Molecules and the Polarizable Continuum Model. *J Phys Chem A* 120:5726–5735. doi:10.1021/acs.jpca.6b05040

334 Bryantsev VS, Mamadou SD, Goddard III WA (2008) Calculation of solvation free energies of
335 charged solutes using mixed cluster/continuum models. *J Phys Chem B* 112:9709–9719.
336 doi:10.1021/jp810292n.

337

338 Choppin GR (1983) Comparison of the solution chemistry of the actinides and lanthanides.
339 *Journal of the Less-Common Metals* 93:323-330. doi:10.1016/0022-5088(83)90177-7

340

341 Choppin GR, Rizkalla EN (1994) *Handbook on the Physics and Chemistry of Rare Earths,*
342 *Solution chemistry of actinides and lanthanides,* Elsevier Science B.V., New York

343

344 Cox R (1981) The excess acidity of aqueous HCl and HBr media. An improved method for the
345 calculation of X-functions and H. *Can J Chem* 59:2023–2028. doi: 10.1139/v81-306

346

347 Cox R (1983) Acidity functions: an update. *Can J Chem* 61:2225–2229. doi: 10.1139/v83-388

348 Cushnie TP, Lamb AJ (2005) Antimicrobial activity of flavonoids. *Int J Antimicrob Agents*
349 26:343-356. doi: 10.1016/j.ijantimicag.2005.09.002

350 doi:10.1016/j.comptc.2017.12.011

351

352 Dunning JrTH (1989) Gaussian basis sets for use in correlated molecular calculations. I. The
353 atoms boron through neon and hydrogen. *J Chem Phys* 90:1007-1023. doi: 10.1063/1.456153

354

355 Grebenyuk SA, Perepichka IF, Popov AF (2002) Evaluation of the parameters of 1:1 charge
356 transfer complexes from spectrophotometric data by non-linear numerical method.
357 *Spectrochim. Acta Part A* 58:2913-2923. doi: 10.1016/S1386-1425(02)00035-5

358

359 Grimme S, Antony J, Ehrlich S, Krieg HA (2010) A consistent and accurate ab initio
360 parametrization of density functional dispersion correction (DFT-D) for the 94 elements H-Pu.
361 *J Chem Phys* 132:154104. doi: 10.1063/1.3382344.

362

363 Hoyuelos FJ, Garcia B, Ibeas S, Munoz MS, Navarro AM, Penacoba I, Leal JM (2005)
364 Protonation Sites of Indoles and Benzoylindoles. *Eur J Org Chem* 6:1161–1171.
365 doi:10.1002/ejoc.200400434

366

- 1
2 367 Kasprzak MM, Erxleben A, Ochocki J (2015) Properties and applications of flavonoid metal
3 368 complexes. RSC Advance 5:45853-45877. doi: 10.1039/C5RA05069C
4 369
- 5 370 Kessler M, Ubeaud G, Jung L (2003) Anti- and pro-oxidant activity of rutin and quercetin
6 371 derivatives. J Pharm Pharmacol 55:131-142. doi: 10.1211/002235702559
7 372
- 8
9 373 Kopacz M (2003) Quercetin- and Morinsulfonates as Analytical Reagents. Journal of
10 374 Analytical Chemistry 58:225-229. doi: 10.1023/A:1022630319311
11 375
- 12
13 376 Le Marchand L (2002) Cancer preventive effects of flavonoids--a review. Biomed
14 377 Pharmacother 56:296-301. doi : 10.1016/S0753-3322(02)00186-5
15 378
- 16
17 379 Leggett DJ (1985) Computational Methods for the Determination of Formation Constants,
18 380 Plenum Press, New York
- 19
20 381 Lutoshkin MA, Kazachenko AS (2017) Assessment of various density functionals and
21 382 solvation models to describe acid-base, spectral and complexing properties of thiobarbituric
22 383 and barbituric acids in aqueous solution. Journal of Computational Methods in Sciences and
23 384 Engineering 17:1-13. doi:10.3233/JCM-170745
24 385
- 25
26 386 Lutoshkin MA, Petrov AI, Kazachenko AS, Kuznetsov BN, Levdansky VA (2018)
27 387 Complexation of rare earth metals by quercetin and quercetin-5'-sulfonic acid in acidic aqueous
28 388 solution. Main Group Chemistry 17:17-25. doi: 10.3233/MGC-180253
29 389
- 30
31 390 M Samsonowicz, Regulska E (2017) Spectroscopic study of molecular structure, antioxidant
32 391 activity and biological effects of metal hydroxyflavonol complexes. Spectrochim Acta A Mol
33 392 Biomol Spectrosc 173:757-771. doi: 10.1016/j.saa.2016.10.031
34 393
- 35
36 394 Manach C, Morand C, Crespy V, Demigne C, Texier O, Régéat F, Rémésy C (1998) Quercetin
37 395 is recovered in human plasma as conjugated derivatives which retain antioxidant properties.
38 396 FEBS Lett 426:331-336. doi: 10.1016/S0014-5793(98)00367-6
39 397
- 40
41 398 Marenich AV, Cramer CJ, Truhlar DG (2009) Universal solvation model based on solute
42 399 electron density and on a continuum model of the solvent defined by the bulk dielectric constant
43 400 and atomic surface tensions. J Phys Chem 113:6378-6396. doi: 10.1021/jp810292n.
44
45
46
47
48
49
50
51
52
53
54
55
56
57
58
59
60
61
62
63
64
65

401

402 Nagimova AD, Zhusupova GE, Erzhanova MS (1996) Synthesis of biologically active bromine
403 derivatives of quercetin. *Chemistry of Natural Compounds* 32:695-697.

404 Panche AN, Diwan AD, Chandra SR (2016) Flavonoids: an overview. *J Nutr Sci* 5:1-15.
405 doi:10.1017/jns.2016.41

406

407 Perdew JP, Ruzsinszky A, Csonka GI, Constantin LA (2011) Workhorse Semilocal Density
408 Functional for Condensed Matter Physics and Quantum Chemistry. *Phys Rev Lett* 106:179902-
409 179906. doi: 10.1103/PhysRevLett.103.026403

410

411 Schmidt MW (1993) General atomic and molecular electronic structure system. *Comput Chem*
412 14:1347-1363. doi: 10.1002/jcc.540141112

413

414 Sotnikova R, Nosalova V, Navarova J (2013) Efficacy of quercetin derivatives in prevention of
415 ulcerative colitis in rats. *Interdiscip Toxicol* 6:9-12. doi: 10.2478/intox-2013-0002

416

417 Srinivas K, King JW, Howard LR, Monrad JK (2010) Solubility and solution thermodynamic
418 properties of quercetin and quercetin dihydrate in subcritical water. *J Food Eng* 100:208-218.
419 doi: 10.1016/j.jfoodeng.2010.04.001

420

421 Tiwari S, Ghosh KK (2010) Mixed micellization properties of cationic monomeric and gemini
422 surfactants. *J Chem Eng Data* 55:4162-4167. doi: 10.1021/je100113r

423

424 Vinayagam R, Xu B (2015) Antidiabetic properties of dietary flavonoids: a cellular mechanism
425 review. *Nutrition & Metabolism* 12 :60-80. doi: 10.1186/s12986-015-0057-7

426

427 Vukovic S, Hay BP, Bryantsev VS (2015) Predicting Stability Constants for Uranyl Complexes
428 Using Density Functional Theory. *Theor Inorg Chem* 54:3995-4001.
429 doi:10.1021/acs.inorgchem.5b00264

430

431 Woźnicka E, Zapała L, Pieniążek E, Kosińska M, Ciszkowicz E, Lecka-Szlachta K, Pusz J,
432 Maciołek U, Dronka J (2017) Synthesis, characterization and antibacterial studies of Tm(III),
433 Yb(III) and Lu(III) complexes of morin. *J Coord Chem* 70:1451-1463.
434 doi:10.1080/00958972.2017.1291935

1
2
3
4
5
6
7
8
9
10
11
12
13
14
15
16
17
18
19
20
21
22
23
24
25
26
27
28
29
30
31
32
33
34
35
36
37
38
39
40
41
42
43
44
45
46
47
48
49
50
51
52
53
54
55
56
57
58
59
60
61
62
63
64
65

1 435 Yanai T, Tew DP, Handyb NC (2004) A new hybrid exchange-correlation functional using the
2 436 Coulomb-attenuating method (CAM-B3LYP). *Chemical Physics Letters* 393:51–57. doi:
3 437 10.1016/j.cplett.2004.06.011
4
5 438
6
7 439 Zhao Y, Truhlar DG (2008) The M06 suite of density functionals for main group
8
9 440 thermochemistry, thermochemical kinetics, noncovalent interactions, excited states, and
10
11 441 transition elements: two new functionals and systematic testing of four M06-class functionals
12
13 442 and 12 other functionals. *Theor Chem Account* 120:215–241. doi: 10.1007/s00214-007-0310-
14 443 x.
15
16 444
17
18 445
19
20 446
21
22 447
23
24 448
25
26 449
27 450
28
29 451
30
31 452
32
33 453
34
35 454
36
37 455
38
39 456
40
41 457
42
43 458
44
45 459
46
47 460
48
49 461
50
51 462
52
53 463
54
55 464
56
57 465
58
59 466
60
61 467
62
63 468
64
65

Table 5. Conditional (K'), "true" (K) stability constants and value of extinction at 429 nm for BQR-Ln(III) systems

Ln(III)	pH \pm 0.01	logK' \pm 0.01	log $\epsilon^{429} \pm$ 0.03	logK \pm 0.05
Ce	5.20	2.18	4.14	4.04
Pr	5.20	2.31	4.14	4.83
Nd	5.20	2.13	4.17	4.27
Sm	5.20	2.59	4.12	4.91
Eu	5.40	2.72	4.13	4.83
Gd	5.20	2.64	4.14	4.82
Tb	4.60	2.43	4.15	5.50
Dy	4.60	2.24	4.16	5.27
	4.40	2.24	4.14	5.43
Er	4.60	2.40	4.18	5.40
	4.80	2.65	4.12	5.47
Tm	4.60	2.26	4.19	5.27
	4.20	2.12	4.14	6.40
Yb	4.40	2.34	4.15	6.42
	4.60	2.58	4.11	6.48
Lu	4.60	2.70	4.14	5.77

Table 4. The results of quantum-chemical simulation.

Density		Dissociation process		
Functional	$\Delta G^{\text{gas}} + \Delta G^{\text{solv.}}$, kJ/mol	ΔE^{ZPE}	$\text{pK}_a(\text{calc})$	$\text{pK}_a(\text{exp})$
PBE0	91.23	-33.99	9.66	
revTPSS	104.79	-32.03	12.39	
M06-L	99.37	-34.05	11.08	
M06	82.97	-33.94	8.25	5.86
M06-2X	82.71	-34.30	8.12	
M06-HF	65.30	-33.86	5.15	
CAM-B3LYP	117.59	-33.56	9.74	
Density		Protonation process		
Functional	$\Delta G^{\text{gas}} + \Delta G^{\text{solv.}}$, kJ/mol	ΔE^{ZPE}	$-\text{pK}_H(\text{calc})$	$-\text{pK}_H(\text{exp})$
PBE0	-27.81	10.84	3.33	
revTPSS	-90.19	2.20	15.77	
M06-L	30.08	8.42	-6.39	
M06	31.35	7.70	-6.48	3.50
M06-2X	25.39	7.91	-5.47	
M06-HF	-81.32	7.83	13.23	
CAM-B3LYP	26.81	-12.60	-2.13	

Table 3. The calculated absolute (a.u.) and relative ($\text{kJ}\cdot\text{mol}^{-1}$) energies of BQR tautomers

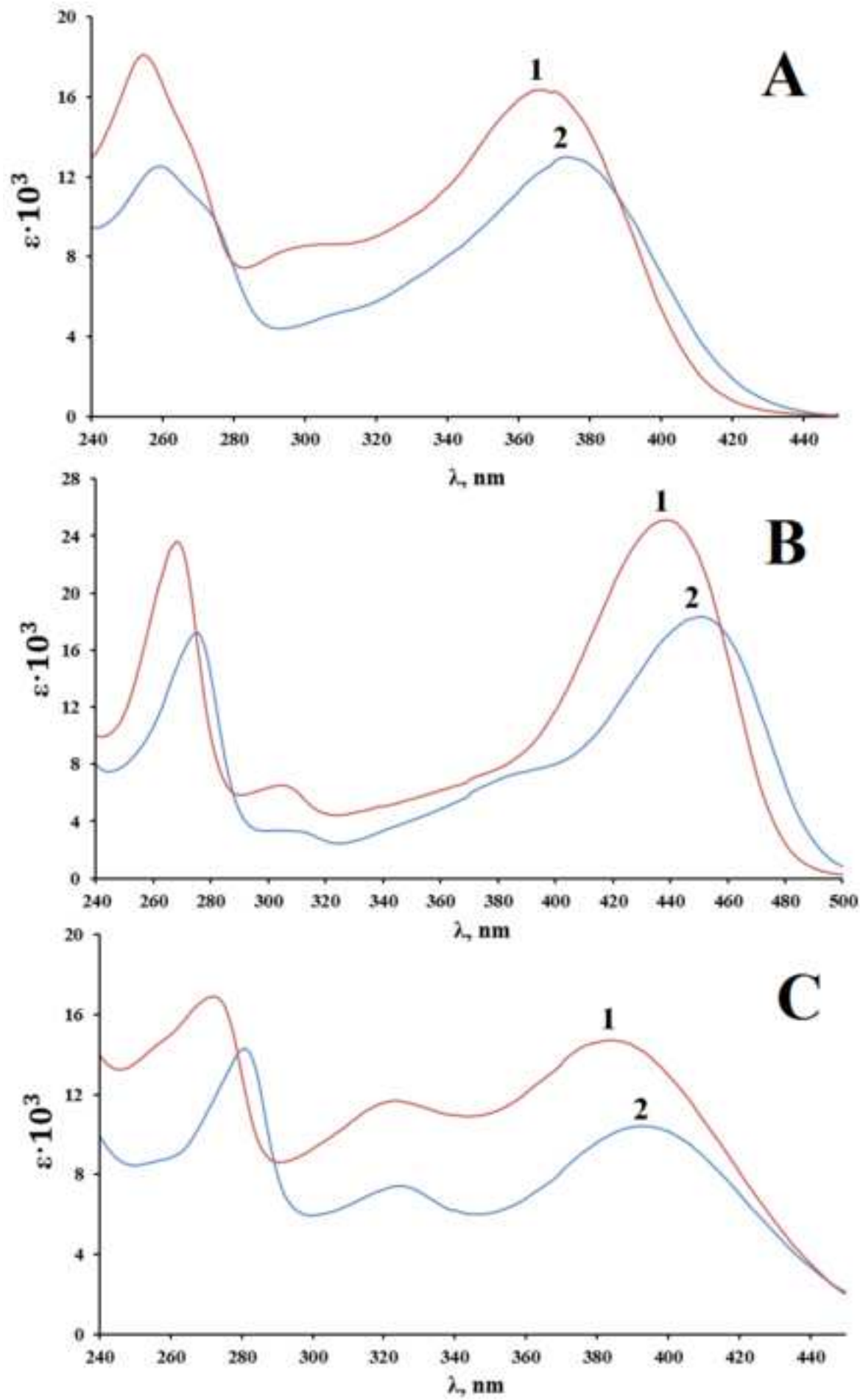
Tautomer	Protonated form (n=2)		Anionic form (n=0)	
	Absolute energy	Relative energy	Absolute energy	Relative energy
N1	-3676.724254	92.19	-3675.946043	0.00
N2	-3676.740029	50.77	-3675.931125	39.17
N3	-3676.740148	50.46	-3675.931271	38.78
N4	-3676.747360	31.53	-3675.922961	60.60
N5	-3676.737160	58.31	-3675.937402	22.69
P1	-3676.759367	0.00		
P2	-3676.711874	124.69		

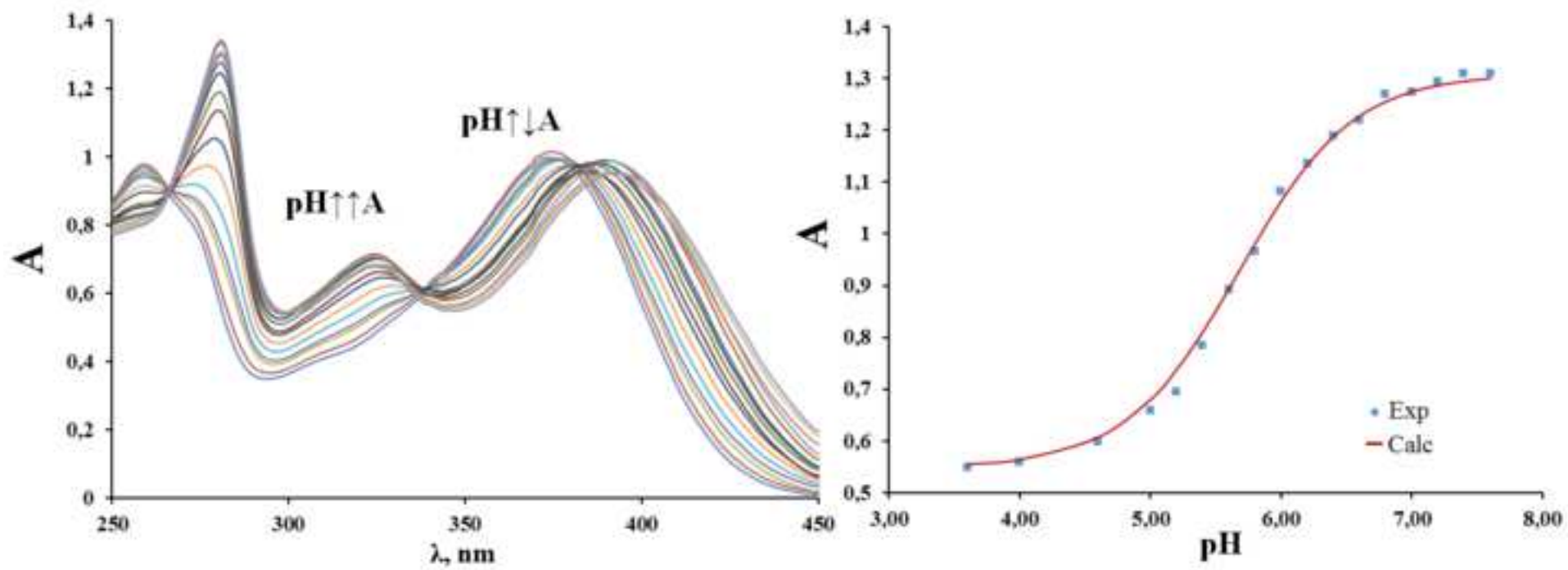
Table 2. The values of pK_a , extinctions of anionic and neutral form of BQR

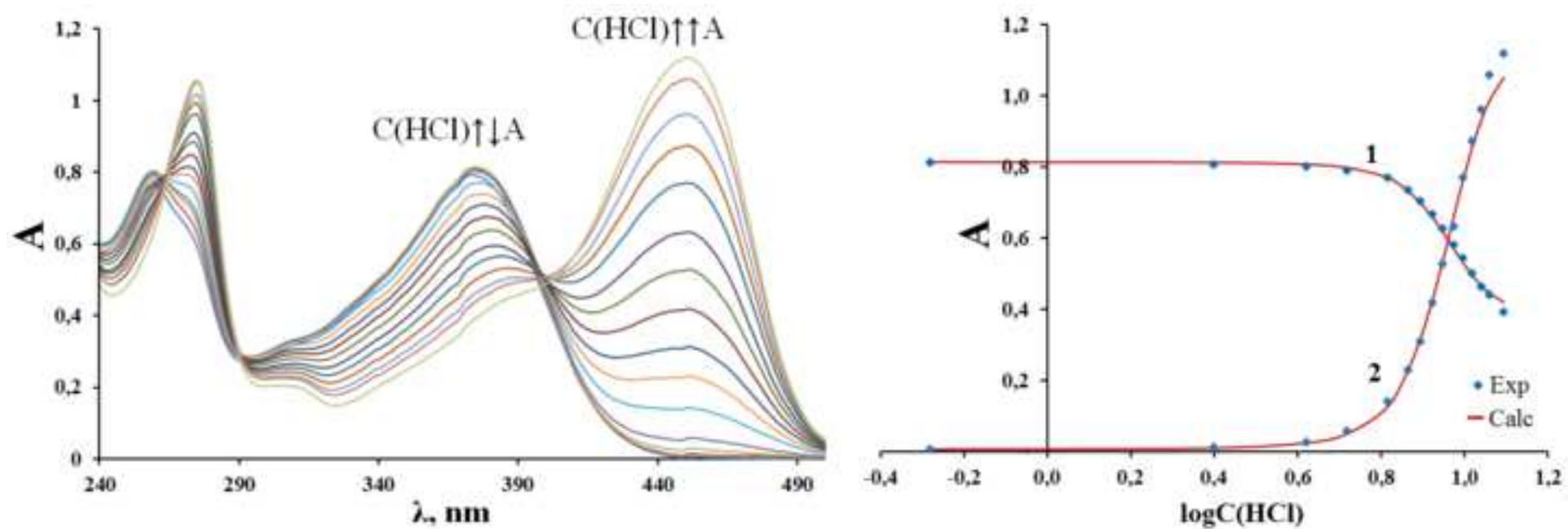
I (NaClO ₄)	0.1		0.5		1.0	
λ , nm	281	408	281	408	281	408
$pK_a \pm 0.02$	5.68	5.70	5.85	5.90	6.04	6.01
$\log(\epsilon_{L-}) \pm 0.01$	4.16	3.96	4.14	3.94	4.14	3.93
$\log(\epsilon_{HL}) \pm 0.01$	3.78	3.60	3.78	3.61	3.79	3.62

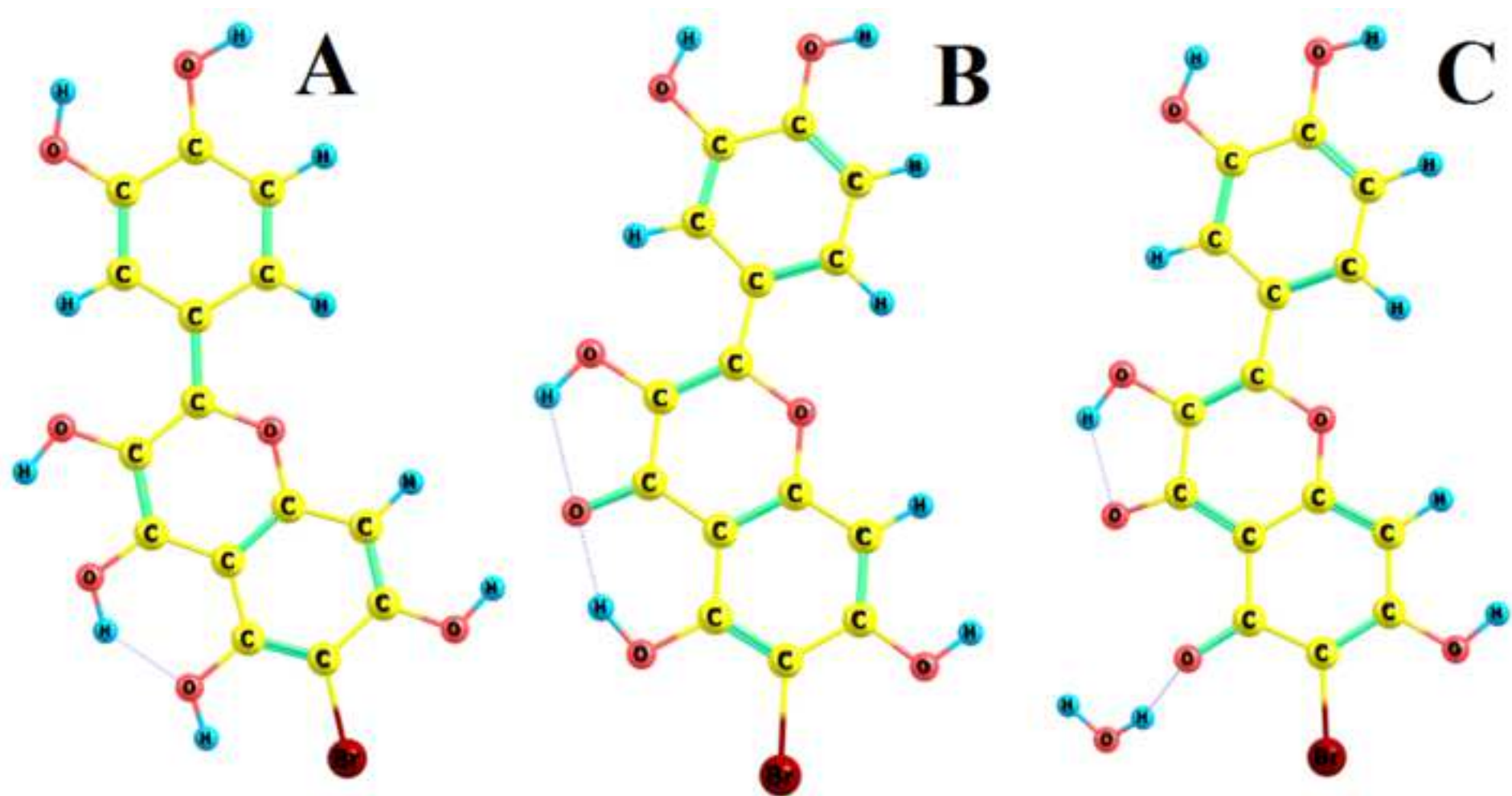
Table 1. The values of wavelength (nm) of main absorbance peaks of BQR and quercetin

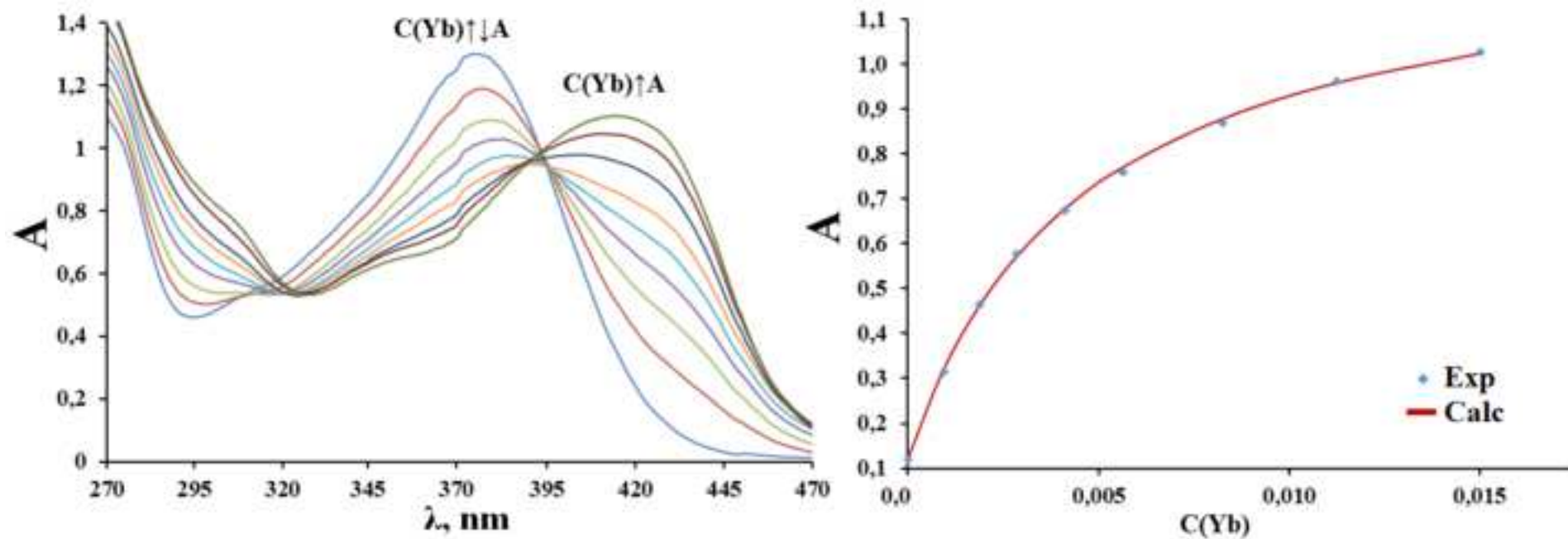
Form	6-Bromoquercetin		Quercetin	
	$\lambda^{\max, 1}$	$\lambda^{\max, 2}$	$\lambda^{\max, 1}$	$\lambda^{\max, 2}$
Neutral	256	373	255	367
Protonated	275	450	268	439
Monoanionic	281	393	272	383

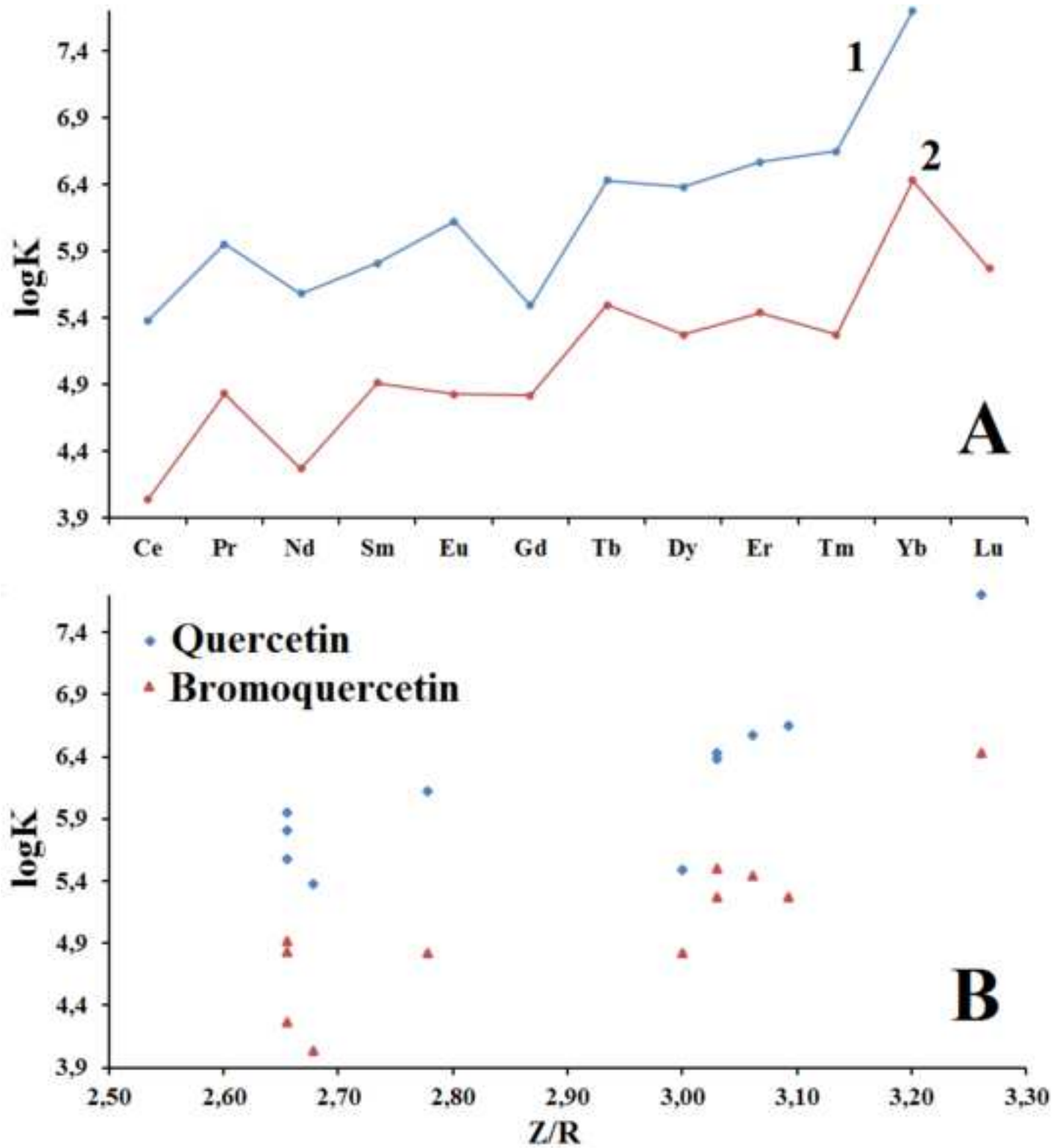


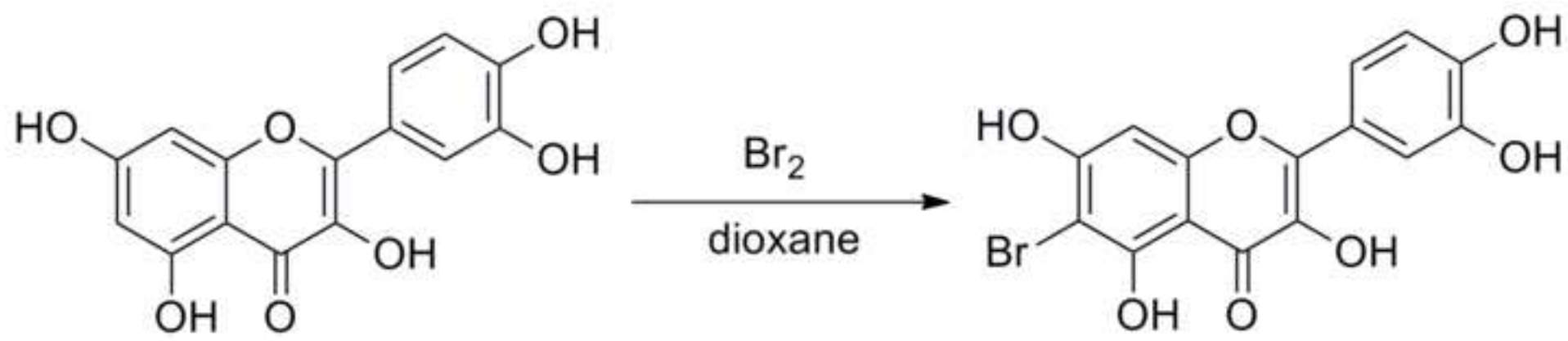


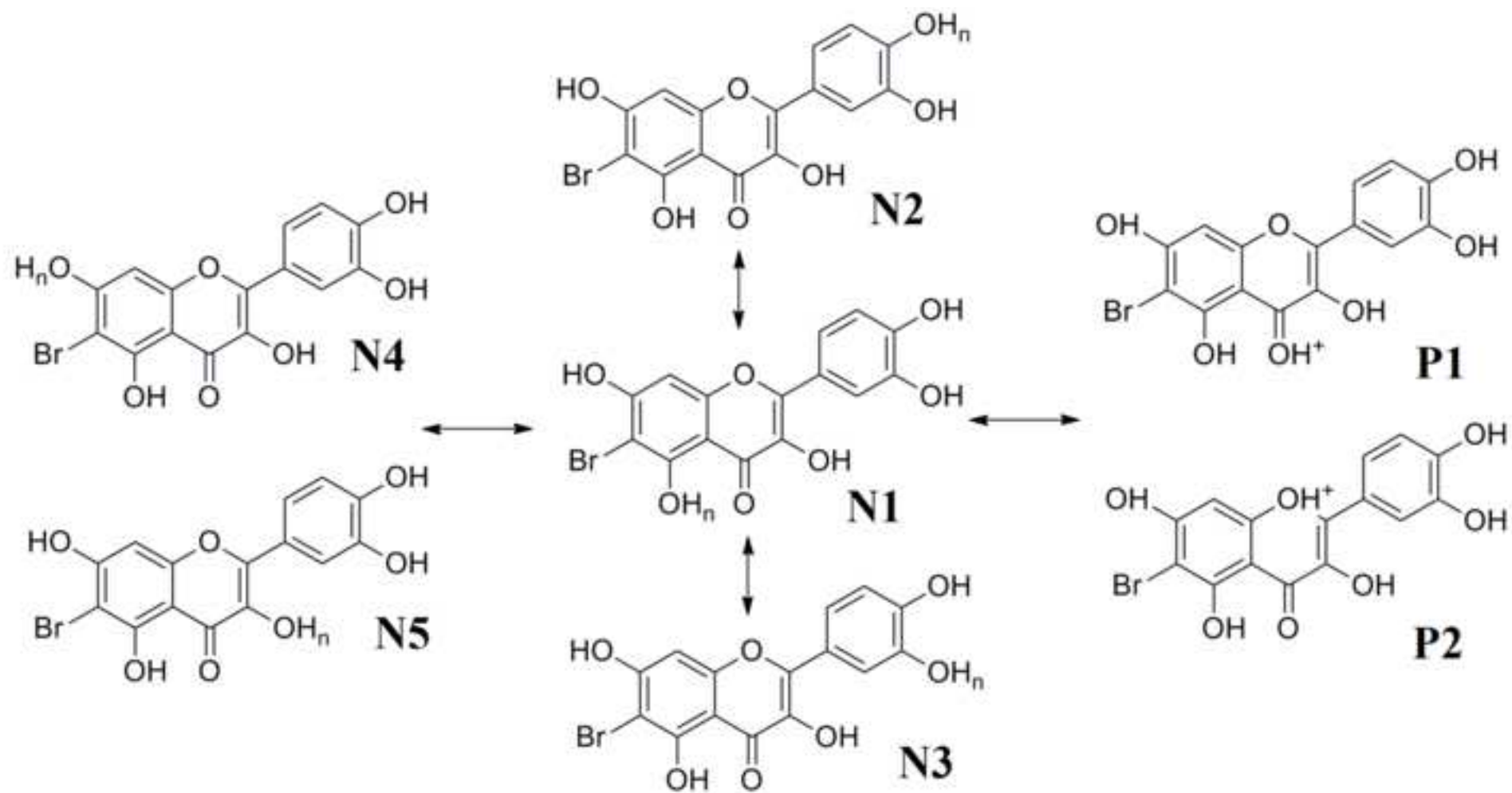


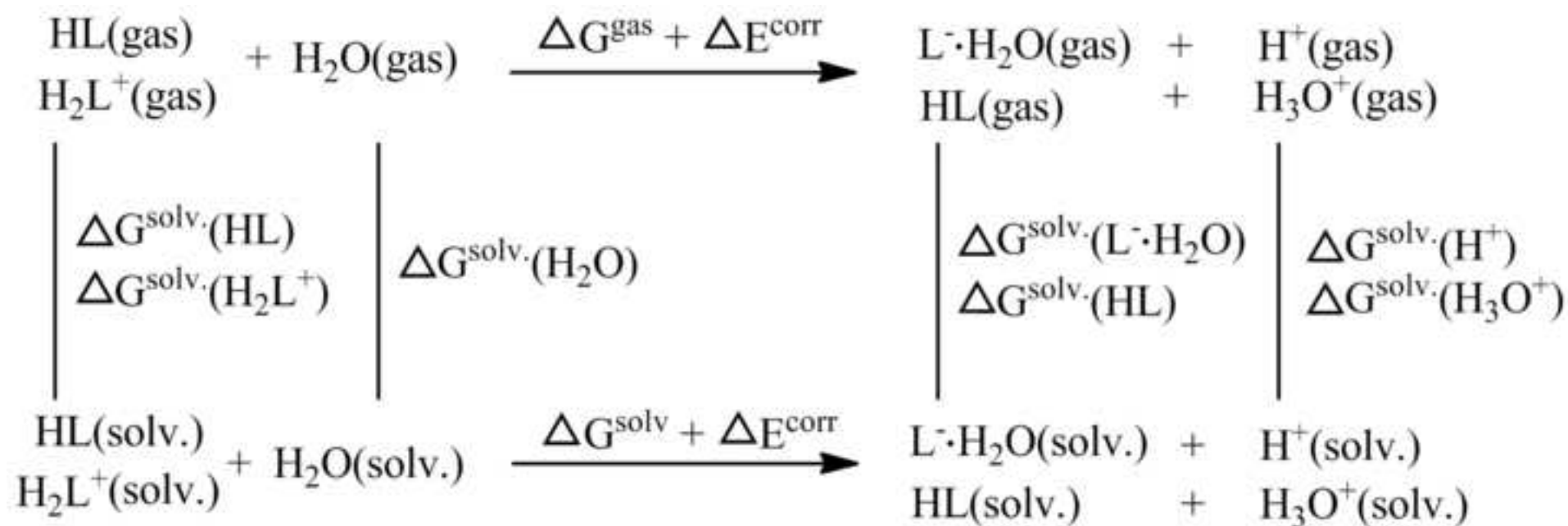


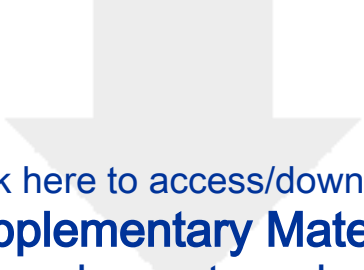












Click here to access/download
Supplementary Material
Supplementary.docx

